

SHS (Self-sustained high-temperature synthesis) of intermetallic compounds: effect of process parameters by computer simulation

Silvia Gennari, Filippo Maglia*, Umberto Anselmi-Tamburini, Giorgio Spinolo

INSTM, IENI/CNR, and Department of Physical Chemistry, University of Pavia, Viale Taramelli, 16, I 27100 Pavia, Italy

Abstract

The very wide temperature ranges and the many different chemical and phase transformation steps experienced by an SHS process make the search for a unifying theory impractical and a numerical approach highly desirable. The work describes an investigation of the $\text{Al} + \text{Ni} \rightarrow \text{AlNi}$ SHS by a computer simulation method developed by the Authors and based on a finite difference numerical engine coupled to a detailed description of several assumed reaction steps. The model includes Al melting, Ni diffusion-controlled dissolution (and possibly Ni melting), nucleation and precipitation of AlNi, and eutectic deposition. The results are discussed from the point of view of feasibility of the process, transition from self-propagating to thermal explosion behavior, and influence of process variables such as reactant grain sizes, diffusion coefficient, initial composition, and thermal conductivity.

© 2003 Elsevier Ltd. All rights reserved.

Keywords: A. Nickel aluminides, based on NiAl; C. Reaction synthesis

1. Introduction

Self-propagating high-temperature synthesis (SHS, or Combustion Synthesis) is now a well-established synthetic technique, extensively used in the last 30 years to synthesize several simple inorganic solids (among which are many intermetallic compounds) as single phases, composites, or functional gradient materials [1–7]. The method is essentially based on the availability of a heterogeneous and sufficiently exothermic chemical reaction to produce (after ignition with an external energy pulse) a reaction front steadily propagating as a thermal and chemical wave through the heterogeneous mixture of the reactants. Advantages of the SHS are its low cost, the simplicity of the apparatus, and fast processing. Concerning intermetallics, these are coupled to favorable properties of the products so obtained in high- T structural applications, in hydrogen storage, and for thermoelectric and magnetic devices [8].

Compared to conventional gas combustion, SHS has the complexity of condensed phase processes and assessing its chemical mechanisms still represents a challenging task. On one side, most theoretical approaches

assume that a single mechanism is rate determining (which seems unreasonable when considering the extremely wide ranges of temperatures, thermal gradients, and chemical potentials experienced by a real SHS), which sometimes is also modeled with gas-phase-type kinetics, a feature unable to account for the marked particle-size effects typically shown by SHS. On the other side, *direct* investigation methods are scarcely available and only *indirect* insights are provided by phase and composition analysis or microscopic inspection of the samples at the end of the process or after quenching, and by in situ investigations of macrokinetics (observation of the propagation mode, determination of time and space profiles of temperature, and of wave velocity). Computer simulation therefore plays here an important role for assessing or discarding the assumed mechanisms, and for suggesting further experiments. As most kinetic parameters are not known in advance, computer simulation is typically used to determine the *trend* of the scarce experimentally measurable quantities as a function of process variables (the variables that it is actually possible to change from experiment to experiment).

The aim of this work is to present the results of a computer simulation approach to the SHS of AlNi from the elements, based on a particular implementation of a flexible and general simulation method especially developed for investigating the chemical mechanisms of SHS

* Corresponding author. Tel.: +39-038-250-7208; fax: +39-038-250-7575.

E-mail address: filippo@chifis.unipv.it (F. Maglia).

processes. The SHS in this system is, to our knowledge, one of the few examples where the SHS mechanism has been experimentally investigated in detail [9–12]. In particular, Fan et al. [9], using the combustion front quenching method, have shown that the reaction starts with Al melting without previous solid state interactions and propagates with a simple dissolution–precipitation mechanism. Only AlNi is formed during the reaction and no other Al–Ni compounds appear as intermediate products; the combustion temperature is above the melting point of Ni but slightly below the melting point of AlNi (in agreement with [10]), and the propagation speed is around 10 mm/s.

The above picture holds as long as SHS on low green density compacts is considered. The scenario drastically changes when other experimental conditions are explored, such as the self-propagating reactions in laminated Al–Ni foils ensembles [12,13], or for high density powder compacts which generally react in the so-called thermal explosion mode, where the reacting pellet uniformly preheats due to its higher thermal conductivity and the combustion is initiated at the ignition temperature simultaneously throughout the entire sample. The effect of compaction degree on thermal conductivity of Al–Ni powder compacts has been investigated by Miura et al. [14]. They have pointed out that the thermal conductivity of a powder Al + Ni mixture can be reduced by almost two orders of magnitude relative to its bulk value as the compact density is reduced below 40%. In this regard, we have reported in our previous work [15] that a thermal conductivity much lower than its theoretical bulk value is necessary to obtain, by computer simulation, a steady propagating SHS.

2. Results and discussion

2.1. Computational model and modeling parameters

We refer to our previous papers for a full description of the computational method [16], and its application to the $Zr + O_2$ SHS of zirconia, for examples to predict the feasibility and dynamic behavior of an SHS and dependence from process variables [17], as well as for the detailed aspects of the particular implementation to the SHS of intermetallic compounds [15].

The method is essentially based on the uncoupling between micro- and macro-kinetic aspects. The former aspect describes the behavior of the system at the level of the grains of the solid phases, takes care of the chemistry (phase transformations and chemical reactions), and can be divided at will into various steps. Each step can, in turn, be described with one or more kinetic laws (i.e. one or more *mechanisms*) or ‘without kinetics’ (i.e. on the basis of enthalpy balance alone).

Significant micro-kinetic variables are the temperature and the conversion degrees of the various chemical steps, which are functions of time.

The macro-kinetic level is based on the system:

$$\begin{cases} \frac{\partial T}{\partial t} = \frac{1}{C} \frac{\partial}{\partial x} \left(\chi \cdot \frac{\partial T}{\partial x} \right) + \frac{2 \cdot \sigma \cdot \varepsilon \cdot (T^4 - T_a^4)}{R \cdot C} + \frac{\dot{q}_{chem}}{C} \\ \dot{q}_{chem} = f(x, T, t) \end{cases}$$

where C is the heat capacity per unit volume, χ is the thermal conductivity, while other symbols are explained below. The first equation (a 1D version of Fourier equation) deals with continuous functions (of time *and* space) that are directly related to the micro-kinetic variables (with the conversion degrees controlling heat sources or sinks) and is solved within a finite differences (FD) scheme. At each discrete time slicing, (1) a Crank Nicholson FD algorithm [18] updates the temperatures at each space interval, then (2) a ‘chemical’ routine updates the advancement degrees of the various assumed steps, possibly modifies the temperatures, and calculates the associated amounts of energy released or absorbed (\dot{q}_{chem}). The last value is in turn used by FD the next time.

Specific assumptions for the $Al(s) + Ni(s) \rightarrow AlNi(s)$ SHS are as follows:

- the SHS is described by a one-dimensional model with a sample in form of a cylinder of radius R ($R = 10$ mm), which loses heat by radiation at the external surfaces (σ is the Stefan–Boltzmann constant and ε is the emissivity, here taken as $\varepsilon = 0.99$);
- the sample is initially made of spherical, equally sized, and uniformly distributed Ni particles embedded in a continuous solid Al pool;
- in the Al–Ni phase diagram, only one compound (AlNi) and two eutectic points, one between pure Al and AlNi and one between AlNi and pure Ni, are considered. The former occurs not much below the melting temperature of the metal (902 K) and has a composition corresponding to $Al_{0.91}Ni_{0.09}$. The enthalpies for pure reactants and for AlNi are modeled with a simple linear dependence from temperature within the range of existence of each pure phase; the thermodynamic functions for the liquid phase are available from literature [19]; the detailed data are reported in a previous work [15]; the aim of this strongly simplified thermodynamic model is to provide a simple (and computationally fast) but consistent way of reproducing the melting points of reactants and product and an adiabatic temperature

‘not much lower’ than the melting point of the compound;

- only *starting* compositions $x \leq 0.5$ are considered for algorithmic reasons (x = mole fraction of Ni);
- the chemical steps considered are: (a) melting of Al, (b) diffusion-controlled dissolution of solid nickel into the molten pool, (c) (possible) melting of Ni, (d) precipitation and melting of the compound, (e) deposition of the eutectic mixture of Al + AlNi;
- solid Ni dissolution into liquid (b) occurs only after complete Al melting, is controlled by Ni diffusion from the solid/liquid interface into bulk liquid, and is described by an invariant-field approximation of the solution of the underlying diffusion equation (unavailable in analytic form) [20] as:

$$r^2 = r_0^2 - kDt,$$

(r is the radius of the particle at a given time, r_0 is its initial value, and k depends on liquid composition at the particle–liquid interface and bulk liquid composition) with:

$$D = D_0 \cdot e^{-\frac{E_a}{RT}} \quad E_a = 76 \text{ kJ mol}^{-1}, \quad D_0 = 10^{-4} \text{ m}^2 \text{ s}^{-1}$$

The numerical values for activation energy (E_a) and pre-exponential term (D_0) have been obtained by comparing experimental data from our group [21] and literature data [11,12];

- all other steps are controlled only by energy transport, and are accounted for at the macro level.

2.2. Effect of process variables on combustion behavior

Fig. 1 shows the space evolution of the thermal SHS wave, at time intervals of 0.02 s, for an almost stoichiometric starting mixture ($x = 0.49$), a grain size of 10 microns, and for the lowest thermal conductivity value at which the reaction can be ignited (i.e. $\chi = \chi_{\text{bulk}}/70$, where χ_{bulk} is calculated from pure phase values [22] and linear dependence from composition). The reaction front propagates steadily with a combustion peak temperature of 1900 K that is just below the melting temperature of the compound, while propagation velocity is about $0.08 \text{ m} \cdot \text{s}^{-1}$, hence in good agreement with experimental measurements [10–12].

The agreement concerning both dynamic behavior, wave velocity, and combustion temperature values between simulations based on reliable input data and experiment information make us confident of the general guidelines of the model. Now, the dependence of wave velocity and combustion temperature and of the propagation modes can be systematically studied by varying the process parameters which can in fact also be controlled experimentally. Process parameters that have been explored independently one from the other in this work are:

- thermal conductivity
- initial composition (Ni mole fraction in the starting powder mixture)
- pre-exponential term of the diffusion coefficient
- grain size

Thermal conductivity (χ) is probably, as previously pointed out, the most important parameter in defining

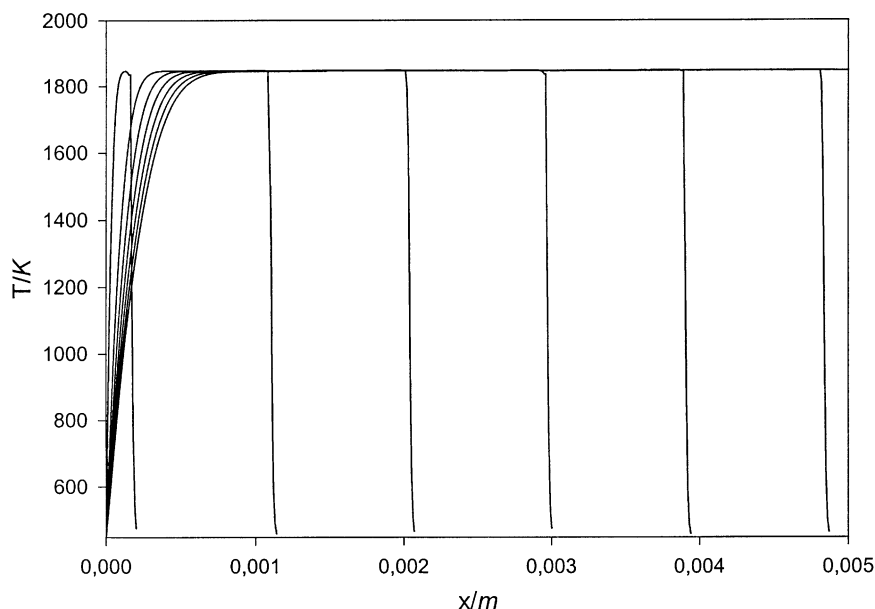


Fig. 1. Space profiles of temperature at different times for a starting composition of 0.49 (Ni molar fraction).

the combustion behavior. Figs. 2 and 3 show how thermal conductivity influences respectively propagation velocity values and propagation mode. Fig. 2 shows how the average value of wave velocity changes as thermal conductivity is varied over three orders of magnitude relatively to the bulk value (χ_{bulk}). As χ is raised from the lowest values ($\chi = \chi_{\text{bulk}}/70$) to the bulk value ($\chi = \chi_{\text{bulk}}$), the wave velocity increases from values typical of an SHS on low density powder compacts to values which are typical of self-propagating reactions in laminated Ni–Al foil ensembles ($v \sim 0.6 \text{ ms}^{-1}$) [12,13]. Moreover, raising the χ value changes the propagation mode from a stationary combustion, with a unique

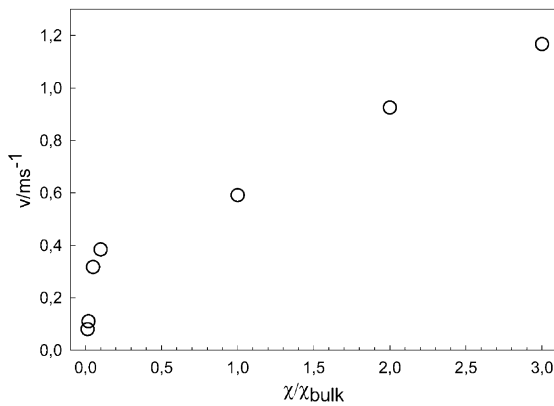


Fig. 2. Wave velocity as a function of thermal conductivity χ ($r_0 = 10 \mu\text{m}$, $D_0 \text{ m}^2\text{s}^{-1} = 10^{-4}$, Ni molar fraction = 0.49).

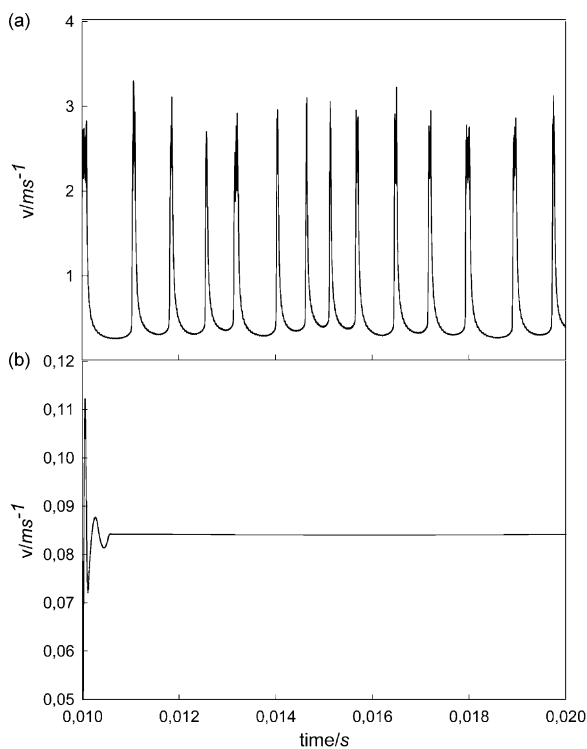


Fig. 3. Time evolution of wave velocity for two significant values of thermal conductivity: $\chi = \chi_{\text{bulk}}$ (a), $\chi = \chi_{\text{bulk}}/70$ (b). ($r_0 = 10 \mu\text{m}$, $D_0 \text{ m}^2\text{s}^{-1} = 10^{-4}$, Ni molar fraction = 0.49, for both cases).

speed value (Fig. 3b), to an oscillatory one (Fig. 3a). In the latter case the value of velocity reported in Fig. 2 is a time average over the values shown by Fig. 3a.

Simulations with even higher conductivities (up to ten times χ_{bulk}) indicate a remarkable increase in the oscillations until a thermal explosion regime, for the highest χ value, was found; that means that, at this χ , the sample pre-heats almost in a homogeneous way and reaches the combustion temperature on its whole volume.

Concerning the initial sample composition, the range between 0.46 (which represents the lower limit for ignition), and 0.499 (the exact stoichiometric value of composition, being 0.5 unavailable for computational reasons) has been taken into consideration: both wave velocity and combustion temperature show a clear dependence on the molar fraction, as shown in Fig. 4. With increasing the Ni molar fraction both velocity and temperature increase. This behavior can be easily forecast and explained considering that lower molar fractions correspond to a higher dilution degree and remarkably lower the available $\Delta_{\text{react}}H$. In addition to that, the variation of the composition of the system also

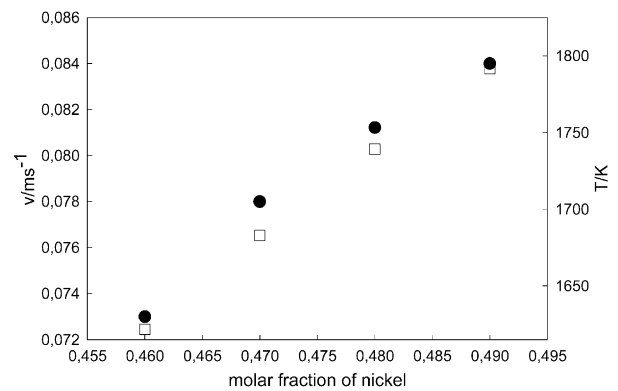


Fig. 4. Wave velocity (black circles) and combustion temperature (white squares) as a function of Ni molar fraction ($\chi = \chi_{\text{bulk}}/70$, $r_0 = 10 \mu\text{m}$, $D_0 \text{ m}^2\text{s}^{-1} = 10^{-4}$).

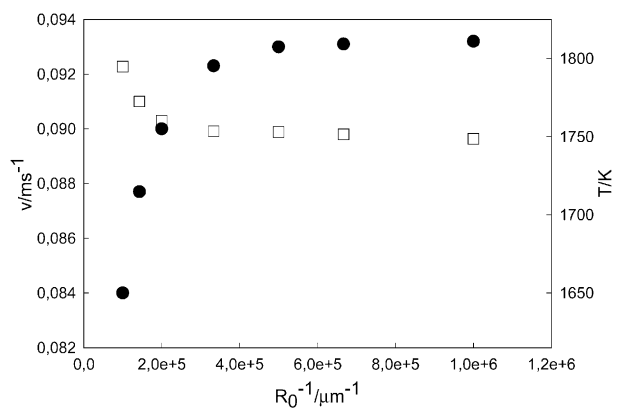


Fig. 5. Wave velocity (black circles) and combustion temperature (white squares) as a function of Ni grain size, r_0 ($\chi = \chi_{\text{bulk}}/70$, Ni molar fraction = 0.49, $D_0 \text{ m}^2\text{s}^{-1} = 10^{-4}$).

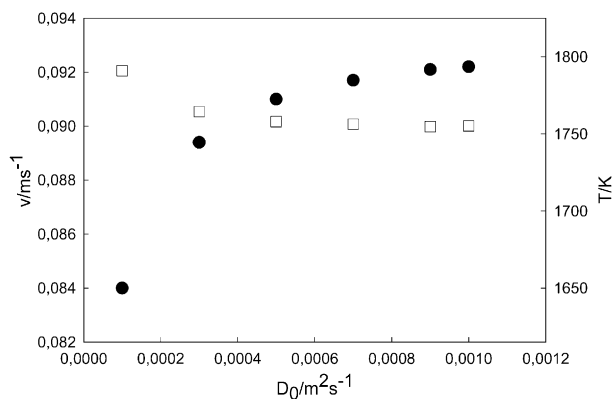


Fig. 6. Wave velocity (black circles) and combustion temperature (white squares) as a function of pre-exponential D_0 of the diffusion coefficient ($\chi = \chi_{\text{bulk}}/70$, $r_0 = 10 \mu\text{m}$, Ni molar fraction = 0.49).

varies the shape of the $H(T)$ function, which further decreases the adiabatic temperature [15].

The dependence of wave velocity and of combustion temperature from grain size is reported in Fig. 5. Only wave velocity (black circles) shows a strong dependence from grain sizes, while combustion temperature (white squares) is practically unmodified: for large grain sizes propagation is obviously slower and shows an almost linear dependence with the inverse of grain size, while a plateau value is reached for smaller grains, down to a micron size. Lower grain sizes were not taken into consideration as they were generally not reachable experimentally.

Direct kinetics effects have also been explored by changing the value of the pre-exponential term of the diffusion coefficient: combustion temperature does not change significantly (Fig. 6), while wave velocity increases rapidly with diffusion coefficient, but seemingly reaches a plateau value for high pre-exponential values.

These last results are representative of the insight provided by computer simulation on the mechanism. A marked dependence of wave velocity from both grain size and diffusion coefficient strongly indicates that the diffusion controlled dissolution of the solid Ni reagent can be considered as rate determining. The onset of a linear dependence of wave velocity from reciprocal of Ni particle size, in particular, is a well known consequence of diffusion control. Our understanding is then

that the attainment of a plateau at smaller grains or higher diffusion coefficients means that diffusion does not affect the SHS any longer, and that we may here speak of a different ‘rate determining mechanism’ because other processes, like precipitation or dissolution of the compound become rate determining. In the model here discussed, no explicit kinetic law is assumed for these processes, which therefore presently appear as indirectly controlled by heat transport. A deeper understanding requires a planned investigation with a more refined model where nucleation and growth of the AlNi product, as well as its dissolution, are explicitly accounted for.

References

- [1] Merzhanov AG, Boroviskaya IP. Dokl Acad Sci USSR (Chem) 1972;204:429.
- [2] Merzhanov AG. Comb Sci Technol 1994;98:307.
- [3] Moore JJ, Feng HJ. Prog Mater Sci 1995;39:243.
- [4] Moore JJ, Feng HJ. Prog Mater Sci 1995;39:275.
- [5] Munir ZA, Anselmi-Tamburini U. Mater Sci Rep 1989;3:277.
- [6] Munir ZA. Am Ceram Soc Bull 1988;67:342.
- [7] Varma A, Lebrat J-P. Chem Eng Sci 1992;47:2179.
- [8] Munir ZA, Odink D. In: Sohn HY, editor. Metallurgical processes of the early twenty-first century. Warrendale, USA: TMS; 1994. p. 167.
- [9] Fan Q, Chai H, Jin Z. Intermetallics 2001;9:602.
- [10] Naiborodenko YuS, Itin VI. Sov Phys J 1973;16:1507.
- [11] Naiborodenko YuS, Itin VI. Combust Explos Shock Wave 1975; 2:343.
- [12] Naiborodenko YuS, Itin VI. Combust Explos Shock Wave 1975; 2:734.
- [13] Anselmi-Tamburini U, Munir ZA. J Appl Phys 1989;66:5039.
- [14] Miura S, Terada Y, Suzuki T, Liu CT, Mishima Y. Intermetallics 2000;8:151.
- [15] Gennari S, Maglia F, Anselmi-Tamburini U, Spinolo G. Journal of Physical Chemistry B 2003;107:732.
- [16] Arimondi M, Anselmi-Tamburini U, Gobetti A, Munir ZA, Spinolo G. J Phys Chem B 1997;101:8059.
- [17] Maglia F, Anselmi-Tamburini U, Gennari S, Spinolo G. Phys Chem Chem Phys 2001;3:489.
- [18] Lapidus L, Pinder G. In: Wiley J, editor. Numerical solution of partial differential equations in science and engineering. New York: Wiley; 1982.
- [19] Grigorovitch KV, Krylov AS. Thermochemica Acta 1998;314:255.
- [20] Aaron HB, Fainstein D, Kotler GB. Appl Phys 1970;41:4404.
- [21] Milanese C. Ph.D thesis, Università di Pavia, 2001.
- [22] Handbook of chemistry and physics, 67th ed. Weast, R.C. editor. Boca Raton, FL: The Chemical Rubber Co. 1986–1987.